Cellular & Molecular Immunology (2017) 14, 293–307

www.nature.com/cmi

RESEARCH ARTICLE

Human fused NKG2D–IL-15 protein controls xenografted human gastric cancer through the recruitment and activation of NK cells

Yan Chen[1,7], Bei Chen[2,7], Ti Yang[1,7], Weiming Xiao[3], Li Qian[1], Yanbing Ding[3], Mingchun Ji[1], Xiaoqun Ge[2] and Weijuan Gong[1,3,4,5,6]

Interleukin (IL)-15 plays an important role in natural killer (NK) and CD8+ T-cell proliferation and function and is more effective than IL-2 for tumor immunotherapy. The trans-presentation of IL-15 by neighboring cells is more effective for NK cell activation than its soluble IL-15. In this study, the fusion protein dsNKG2D–IL-15, which consisted of two identical extracellular domains of human NKG2D coupled to human IL-15 via a linker, was engineered in Escherichia coli. DsNKG2D–IL-15 could efficiently bind to major histocompatibility complex class I chain-related protein A (MICA) of human tumor cells with the two NKG2D domains and trans-present IL-15 to NK or CD8+ T cells. We transplanted human gastric cancer (SGC-7901) cells into nude mice and mouse melanoma cells with ectopic expression of MICA (B16BL6–MICA) into C57BL/6 mice. Then, we studied the anti-tumor effects mediated by dsNKG2D–IL-15 in the two xenografted tumor models. Human dsNKG2D–IL-15 exhibited higher efficiency than IL-15 in suppressing gastric cancer growth. Exogenous human dsNKG2D–IL-15 was centrally distributed in the mouse tumor tissues based on in vivo live imaging. The frequencies of human CD56+ cells infiltrated into the tumor tissues following the injection of peripheral blood mononuclear cells into nude mice bearing human gastric cancer were significantly increased by human dsNKG2D–IL-15 treatment. Human dsNKG2D–IL-15 also delayed the growth of transplanted melanoma (B16BL6–MICA) by activating and recruiting mouse NK and CD8+ T cells. The anti-melanoma effect of human dsNKG2D–IL-15 in C57BL/6 mice was mostly decreased by the in vivo depletion of mouse NK cells. These data highlight the potential use of human dsNKG2D–IL-15 for tumor therapy.
Cellular & Molecular Immunology (2017) **14,** 293–307; doi:10.1038/cmi.2015.81; published online 14 September 2015

Keywords: fusion protein; IL-15; NK cells; NKG2D; tumor

INTRODUCTION

Interleukin (IL)-15 plays an important role in the development, activity, and persistence of natural killer (NK) and $CD8^+$ T cells, indicating that it has great potential to promote anti-tumor immune responses.[1,2] Unlike IL-2, IL-15 does not seem to be involved in the apoptosis of activated effector $CD8^+$ T cells and the induction of $CD4^+CD25^+Foxp3^+$ regulatory T cells.[3,4] Furthermore, preclinical studies suggest that IL-15 is less toxic than IL-2.[5] Previous studies have investigated the anti-tumor activities mediated by membrane-bound IL-15 on NK cells,[6] adenovirus-mediated IL-15 gene transfer,[7,8] or generation of IL-15 and IL-15 receptor alpha fusion proteins to trans-present IL-15.[9,10] IL-15 is among the top listed agents considered

[1]Department of Immunology, School of Medicine, Yangzhou University, Yangzhou 225001, People's Republic of China; [2]Department of Pharmacology, School of Medicine, Yangzhou University, Yangzhou 225001, People's Republic of China; [3]Department of Gastroenterology, The Second Affiliated Hospital, Yangzhou University, Yangzhou 225001, People's Republic of China; [4]Jiangsu Key Laboratory of Integrated Traditional Chinese and Western Medicine for Prevention and Treatment of Senile Diseases, Yangzhou University, Yangzhou 225009, People's Republic of China; [5]Jiangsu Key Laboratory of Zoonosis, Yangzhou University, Yangzhou 225009, People's Republic of China and [6]Jiangsu Co-innovation Center for Prevention and Control of Important Animal Infectious Diseases and Zoonoses, Yangzhou, 225009, People's Republic of China
[7]These authors contributed equally to this article.
Correspondence: W Gong, [1]Department of Immunology, School of Medicine, and [2]Department of Gastroenterology, The Second Affiliated Hospital, and [3]Jiangsu Key Laboratory of Integrated Traditional Chinese and Western Medicine for Prevention and Treatment of Senile Diseases, and [4]Jiangsu Key Laboratory of Zoonosis, Yangzhou University, and [5]Jiangsu Co-innovation Center for Prevention and Control of Important Animal Infectious Diseases and Zoonoses, Yangzhou, 225009, People's Republic of China.
E-mail: wjgong@yzu.edu.cn
Received: 13 November 2014; Revised: 1 August 2015; Accepted: 1 August 2015

by the National Cancer Institute to have high potential for cancer immunotherapy.[11]

IL-15 binds to IL-15Rα with high affinity and forms a complex that shuttles from the endoplasmic reticulum to the cell surface, particularly on monocytes and dendritic cells. IL-15Rα trans-presents IL-15 to the IL-2/15Rβγ common receptor expressed on neighboring cells, although cis-presentation is also possible.[12,13] Trans-presentation of IL-15 is required for the maintenance of several lymphoid cell subsets, such as natural killer, natural killer T, and memory $CD8^+$ T cells.[14,15] The relevance of IL-15 trans-presentation for an efficient anti-tumor response has been demonstrated in mouse models with IL-15Rα-transfected MC38 tumor cells[16] and the use of soluble complexes of recombinant IL-15 with IL-15Rα,[17] soluble IL-15 with IL-15Rα–IgG1-Fc complexes,[18] anti-IL-15 fusion proteins,[19] and anti-IL-15Rα sushi domain–IL-15 fusion proteins.[10,20] The soluble complexes and the fusion proteins were much more stimulatory than IL-15 alone.

NKG2D is an important activating receptor that is widely expressed on NK, $CD8^+$ T, NKT, γδT, and some $CD4^+$ T cells. Following ligation to DAP10 or DAP12, NKG2D induces cytotoxicity and IFN-γ production by NK cells and costimulation of T-cell functions. Major histocompatibility complex class I chain-related protein A/B (MICA/MICB) and the UL-16 binding protein are NKG2D ligands in humans.[21,22] These ligands are preferentially expressed on stress-induced cells or tumor cells and are not found in most normal tissues.[23,24] A biofunctional fusion protein (scFv-NKG2D) that binds tumor cells through NKG2D and recruits and stimulates T cells through an anti-CD3 single-chain variable fragment can significantly suppress tumor growth and efficiently induce immune memory.[25] Thus, NKG2D ligands can serve as targets in tumor-targeted treatments.

We previously generated a mouse dsNKG2D–IL-15 (mdsNKG2D–IL-15) fusion protein,[26] but the trans-presentation of fused dsNKG2D–IL-15 by neighboring cells and the bio-distribution of dsNKG2D–IL-15 in tumor-bearing mice was not fully elucidated. In this study, a human dsNKG2D–IL-15 (hdsNKG2D–IL-15) protein in which two identical extracellular human NKG2D domains were fused to the N-terminus of human IL-15 was generated. Because human NKG2D was not able to bind RAE-1 (the MICA homologue in mice) and other ligands of mouse NKG2D,[25] we characterized the activation of human NK cells by hdsNKG2D–IL-15 trans-presented by neighboring cells *ex vivo* and the activities of hdsNKG2D–IL-15 against xenografted human gastric cancers in nude mice. B16BL6–MICA cells were also transplanted into normal C57BL/6 mice, and the bio-distribution of hdsNKG2D–IL-15, its anti-melanoma activity, and its activation of NK and $CD8^+$ T cells was evaluated in tumor-bearing mice.

MATERIALS AND METHODS

Materials

The plasmid containing the human NKG2D cDNA sequence was provided by Prof. L. L. Lanier of UCLA, and the pORF-hIL-15 plasmid was purchased from *In vivo* Gen (San Diego, CA, USA). *Escherichia coli* strain M15 and the pQE31 plasmid were obtained from Qiagen (Dusseldorf, Germany). *Taq* DNA polymerase, restriction endonucleases, T4 DNA polymerase, PCR product purification kits, and DNA recovery kits were all purchased from Takara Bio (Dalian, China). Ni^+-NTA purification columns were obtained from Qiagen (Dusseldorf, Germany). Recombinant human NKG2D–Ig and the NKG2A antibody (FAB1059A) were purchased from R&D Systems (Boston, MA, USA). Recombinant human IL-15 was obtained from Peprotech (Rocky Hill, NJ, USA).The IL-15 polyclonal antibody (pAb) H-114 was purchased from Santa Cruz Biotechnology (Santa Cruz, CA, USA). The IL-15 conformational monoclonal antibody (mAb) (Ab55276) with or without fluorescent labeling was from Abcam (Cambridge, MA, USA). Antibodies against human MICA (6D4), CD56 (MEM-188), CD16 (CB16), NKG2D (1D11), CD69 (FN50), IFN-γ (4SB3), CD107a (H4A3), NKp46 (9E2), CXCR3 (TG1), and DNAM-1 (11A8) were obtained from BioLegend (San Diego, CA, USA). Antibodies against mouse NK1.1 (PK136), NKG2D (CX5), CD122 (TU27), and CD8 (53.67) were also from BioLegend. Secondary antibodies conjugated to horseradish peroxidase (HRP) or a fluorophore were obtained from Invitrogen (Grand Island, NY, USA). The K562, HeLa, and B16BL6 cell lines were all from ATCC. The human gastric cancer cell line SGC-7901 was obtained from the Chinese Academy of Science. MICA was ectopically expressed on K562[27] or B16BL6[28] cells as previously described.

Construction of the recombinant hdsNKG2D–IL-15 plasmid

The genetic sequences encoding the human NKG2D extracellular domain (Phe78–Val 216) were amplified with two different pairs of primers to generate two NKG2D fragments with different tail sites for restriction enzyme recognition. The sequence of the first primer pair was 5′-CTGGATCCGTTCCTAAACTCATTATTC AACCAAG and 3′-CGAGGCCTAGATCCGCCGCCTCCTG AACCGCCACCTCCTGAGCCGCCTCCGCCTGAGCCA CCGCCTCCCACAGTCCTTTGCATGCAGATGTAC, and the sequence of the second primer pair was 5′-CTAGGCCTTT CCTAAACTCATTATTCAACCAAG and 3′-CTCTGCAGA GATCCGCCGCCTCCTGAACCGCCACCTCCTGAGCCGC-CTCCGCCTGAGCCACCGCCTCCCACAGTCCTTTGCATG CAGATGTAC. Two NKG2D gene segments were sequentially inserted into pQE31. The primers for human IL-15 amplification (Asn 49–Ser 162) were forward: 5′-CTCTGCAGAA CTGGGTGAATGTAATAAGTGATT and reverse: 3′-CG AAGCTTTCAAGAAGTGTTGATGAACATTTGG. The IL-15 gene fragment was inserted into the pQE31 plasmid downstream from the two NKG2D domains. The primers introduced the recognition sites for the restriction enzymes *BamH* I, *Stu* I, *Pst* I, and *Hind* III. Flexible linkers were inserted between the three domains. The mdsNKG2D–IL-15 protein was generated as described previously.

Generation of the hdsNKG2D–IL-15 protein

The fusion protein was produced in bacteria as an inclusion body after IPTG induction. The inclusion body was isolated

and dissolved in urea. The recombinant protein was purified using two Ni^{+}-NTA columns and renatured in a solution of 400 mM L-arginine, 5 mM reduced glutathione, 0.5 mM oxidized glutathione, 100 mM Tris-HCl, 2 mM ethylenediaminetetraacetic acid, 10% glycerin, 0.2 mM phenylmethanesulfonyl fluoride, 0.7 μg mL^{-1} pepstatin A, and 0.5 μg mL^{-1} leupeptin. Then, the protein solution was replaced with PBS. Prior to use, LPS was removed from the recombinant protein samples on and a polymyxin B-modified resin column obtained from GenScript (Nanjing, China). The endotoxin concentration of each sample was below 0.06 EU mL^{-1} in *Limulus* amebocyte lysate tests.

Western blotting

The recombinant human hdsNKG2D–IL-15 protein at 1:1, 1:2, or 1:5 dilutions was separated on 1-mm-thick 5–12% Tris-glycine gels and then transferred to a polyvinylidene fluoride (PVDF) membrane. The PVDF membranes were blocked with 5% (w/v) nonfat dry milk powder in Tris-buffered saline and Tween 20 (TBST) buffer. The anti-NKG2D pAb (Ab96606, Abcam) or anti-IL-15 pAb (Ab134177, Abcam) was diluted 1:500 in TBST buffer containing 2 mg mL^{-1} BSA and incubated with the membrane for 2 h at 37°C. Then, the PVDF membranes were incubated with HRP-conjugated goat anti-rabbit IgG (1:3000 in TBST) (Invitrogen) for 1 h. The membranes were washed extensively with TBST, and immune reactive bands were visualized with a chemiluminescence reagent (Dakewe, Shenzhen, P.R. China).

Enzyme-linked immunosorbent assay (ELISA)

The human NKG2D and IL-15 domains of hdsNKG2D–IL-15 were identified by ELISA assays. Briefly, bovine serum albumin (BSA), human dsNKG2D–IL-15 (1 μg), human NKG2D–Ig (1 μg), and recombinant human IL-15 (1 μg) were coated onto polystyrene foam wells overnight. The primary antibody (10 μg mL^{-1}) against either NKG2D or IL-15 was added, and then a secondary antibody (1 μg mL^{-1}) labeled with HRP was added to the plate. Binding of hdsNKG2D–IL-15 to MICA was confirmed after initially coating the recombinant soluble MICA protein (1 μg) on the wells. Different concentrations of hdsNKG2D–IL-15 (5, 10, and 20 μg mL^{-1}) were added to the plate. Then, the IL-15 antibody and HRP-secondary antibodies were added to the wells. The OD_{450} value was read after adding the substrate and stop solution to the wells.

Competition assay

B16-MICA or B16 mock-transfected cells were incubated with 0, 1, 2, 5, or 10 μg mL^{-1} of human or mouse dsNKG2D–IL-15 at 37°C for 1 h. The cells were collected and washed with PBS. Next, commercial recombinant human NKG2D–Ig (5 μg mL^{-1}) was incubated with these cells at 37°C for another hour. After washing, the cells were stained with fluorescent goat anti-human IgG antibody for 30 min and detected by flow cytometry.

NK cell proliferation

The MTS/PMS assay (Promega, Madison, WI, USA) was used to detect the proliferation of NK cells. NK cells were sorted from peripheral blood mononuclear cells (PBMCs) using a magnetic bead-labeled CD56 antibody (Miltenyi, Germany). The cells were cultured with recombinant soluble human dsNKG2D–IL-15 (10 ng mL^{-1}), immobilized dsNKG2D–IL-15 that was coated on plates (2 μg), or commercialized soluble IL-15 (10 ng mL^{-1}). A sample of NK cells that were cultured alone was used as a control, and the samples were run in triplicate. The MTS/PMS solution was added to each well on day 3. After 4 h, the absorbance was read at 490 nm.

Detection of cytotoxicity

NK cell cytotoxicity was determined by assessing CD107a expression on NK cells or by performing a lactate dehydrogenase (LDH) release assay. PBMCs were mixed with K562 cells at ratios of 3:1, 1:1, and 1:3. Either fluorochrome-conjugated anti-CD107a mAb or an isotype control antibody was added to the mixture for CD107a staining. After 2 h, monensin (GolgiStop; BD Biosciences, San Jose, CA, USA) was added at a 1:100 dilution and incubated for another 2 h. Surface staining was achieved by incubating the cells with an anti-CD56 mAb on ice for 30 min. The cells were washed, re-suspended in PBS, and immediately analyzed by flow cytometry. We assessed the cytotoxicities of NK cells by co-culturing the NK cells with target cells for 4 h and then estimating the cytotoxicity in LDH release assays according to the manufacturer's protocol.

Intracellular staining

IFN-γ production was assessed with an intracellular staining kit (eBioscience, San Diego, CA, USA). Briefly, PBMCs were cultured with soluble dsNKG2D–IL-15, immobilized dsNKG2D–IL-15, or soluble IL-15 in the presence of brefeldin A (10 μg mL^{-1}; eBioscience, San Diego, CA, USA) at 37°C for 4 h. Then, the NK cells were stained with an anti-CD56 mAb by incubating at 4°C for 30 min. The cells were fixed and permeabilized at room temperature for 20 min. The permeabilized cells were stained with either a PE-labeled anti-IFN-γ mAb or the isotype antibody and analyzed by flow cytometry.

Mouse tumor models

We subcutaneously implanted SGC-7901 cells ($n = 6$, 2×10^6 cells) into the backs of nude mice. Human dsNKG2D–IL-15 (60 μg), mdsNKG2D–IL-15 (60 μg), recombinant human IL-15 (60 μg) or PBS was intraperitoneally injected daily into these mice from days 5 to 20.Tumor growth was measured using digital calipers, and the tumor volume was calculated as $V = (\text{width})^2 \times \text{length}/2$. All mice were killed on day 21 for the collection of their spleens and tumors. To evaluate the survival of tumor-bearing mice, we also implanted SGC-7901 cells ($n = 6$, 2×10^6 cells) into the backs of nude mice treated with recombinant proteins or PBS, Mouse viability was recorded daily.

To create B16BL6 cell-transplanted tumor mice, B16BL6 or B16BL6–MICA cells were subcutaneously injected into C57BL/6 mice ($n = 6$, 2×10^6 cells). Human dsNKG2D–IL-15 (60 μg), mdsNKG2D–IL-15 (60 μg), or PBS were intraperitoneally injected daily into these mice from days 5 to 21.Tumor growth was measured daily. All mice were killed on day 22, and their spleens were collected. All experiments were conducted in accordance with the protocols approved by the Institutional Animal Care and Use Committee of Yangzhou University.

In vivo distribution of human dsNKG2D–IL-15

Human dsNKG2D–IL-15 was labeled with cyanine dye 5.5 with 95% purity by Shanghai Kaijin Biotechnology (Shanghai, China). B16-MICA cells (5×10^6) were subcutaneously injected into the backs of C57BL/6 mice ($n = 3$). Ten days later, fluorescent dsNKG2D–IL-15 (80 μg) was injected into the tail vein. Fluorescent signals in mice were captured at 0, 1, 2, 4, 8, 20, and 24 h by the Shimadzu OPT plus imaging system.

Isolation of lymphocytes from tumor tissues

Tumor samples from nude mice were finely grounded, digested with collagenase type III (100 mg mL^{-1}), dispase (550 mg mL^{-1}), and DNase I (300 mg mL^{-1}) for 4–6 h and sieved through 70 μm and 40 μm pore strainers. The cell suspensions were centrifuged and treated with Tris-NH_4Cl to remove red blood cells. The lymphocytes were isolated by centrifugation in a 35% Percoll solution. Lymphocyte suspensions were incubated with mAbs against NK1.1 and NKG2D and detected by flow cytometry.

In vivo depletion of NK and $CD8^+$ T cells

A rabbit polyclonal anti-asialo-GM1 antibody (100 μg) was intraperitoneally injected into C57BL/6 mice or nude mice every 3 days. The injection started 3 days prior to the injection of B16BL6–MICA cells or SGC-7901 cells and lasted throughout the course of the experiment. Similarly, an anti-CD8 antibody (clone 2.43, 200 μg) was repeatedly injected into mice (once per week) to remove $CD8^+$ T cells. Cell depletion was occasionally monitored by analyzing PBMCs by flow cytometry using an NK1.1 or CD8 marker.

Statistical analysis

Differences between the groups were analyzed using Student's *t*-test. Analysis of variance was performed to determine the different effects of various treatment groups. Kaplan–Meier survival curves were plotted and analyzed with GraphPad Prism software. $P < 0.05$ was considered statistically significant.

RESULTS

Binding of human dsNKG2D–IL-15 to MICA

The schematic structure of human dsNKG2D–IL-15 is shown in Supplementary Figure 1a. The recombinant pQE31–hdsNKG2D–IL-15 plasmid was verified by restriction digestion (Supplementary Figure 1b).The purified human dsNKG2D–IL-15 protein was a monomer approximately 43 kD in size (both before and after renaturation), which was consistent with the expected size (Supplementary Figure 1c). The NKG2D and IL-15 domains in human dsNKG2D–IL-15 were identified by binding to their corresponding antibodies in a western blot assay (Figure 1a). Two indirect ELISA assays were developed to determine whether the NKG2D and IL-15 domains of dsNKG2D–IL-15 had a normal structure after renaturation. The antibody against human NKG2D bound to both the recombinant hdsNKG2D–IL-15 and human NKG2D–Ig proteins but did not bind to BSA. The IL-15 antibody bound to hdsNKG2D–IL-15 and human IL-15 but did not bind to BSA (Figure 1b). Thus, the recombinant hdsNKG2D–IL-15 protein generated in *E. coli* was efficiently renatured *in vitro*.

The binding of hdsNKG2D–IL-15 to the NKG2D ligand MICA was measured by a sandwich ELISA assay. DsNKG2D–IL-15 efficiently bound to MICA-coated plates because the addition of the IL-15 antibody or NKG2D polyclonal antibody led to significantly enhanced absorbance in a dose-dependent manner. The lack of binding of the NKG2D monoclonal antibody to dsNKG2D–IL-15 that was pre-associated with plate-bound MICA may be attributed to the fact that the same NKG2D epitope was recognized by MICA and the NKG2D monoclonal antibody (1D11), as shown in an open patent (US7879985). The binding activity was significantly lower when the plates coated with MICA were incubated with mouse dsNKG2D–IL-15 compared with human dsNKG2D–IL-15 (Supplementary Figure 2). Moreover, no human NKG2D pAb binding was detected when RAE-1ε (a ligand of mouse NKG2D) was pre-coated on plates and incubated with human dsNKG2D–IL-15 (Figure 1c). The recombinant human dsNKG2D–IL-15 fusion protein also efficiently bound to the K562–MICA, HeLa, and SGC7901 cells, as shown by flow cytometry with a fluorescence-labeled anti-IL-15 antibody (Figure 1d). The expression of MICA or NKG2D ligands on these tumor cells was confirmed by staining with a MICA-specific mAb (6D4) or commercial recombinant NKG2D–Ig protein as shown in Supplementary Figure 3. Because of the high expression level of MICA on the K562–MICA cells, a low hdsNKG2D–IL-15 concentration (1 μg mL^{-1}) efficiently ligated with membrane-bound MICA. Human dsNKG2D–IL-15 also bound to K562 cells at a high concentration for the baseline expression of MICA on the cells.

We used a melanoma cell line (B16-MICA) in which MICA was ectopically expressed[28] to verify human dsNKG2D–IL-15 binding to cell membrane-bound MICA via the NKG2D domain. B16-MICA cells were pre-incubated with human or mouse dsNKG2D–IL-15, stained with a rabbit pAb against both human and mouse IL-15, and detected using a fluorescent goat anti-rabbit antibody. As expected, human dsNKG2D–IL-15 bound strongly to B16-MICA cells, while mouse dsNKG2D–IL-15 bound weakly to the same cells. When B16-MICA cells were pre-incubated with a MICA antibody, neither human nor mouse dsNKG2D–IL-15 could bind to the B16-MICA cells (Figure 1e). Human and mouse dsNKG2D–IL-15 could not bind to mock-transfected B16 cells (Supplementary Figure 4). Similarly, the NKG2D mAb could not bind to

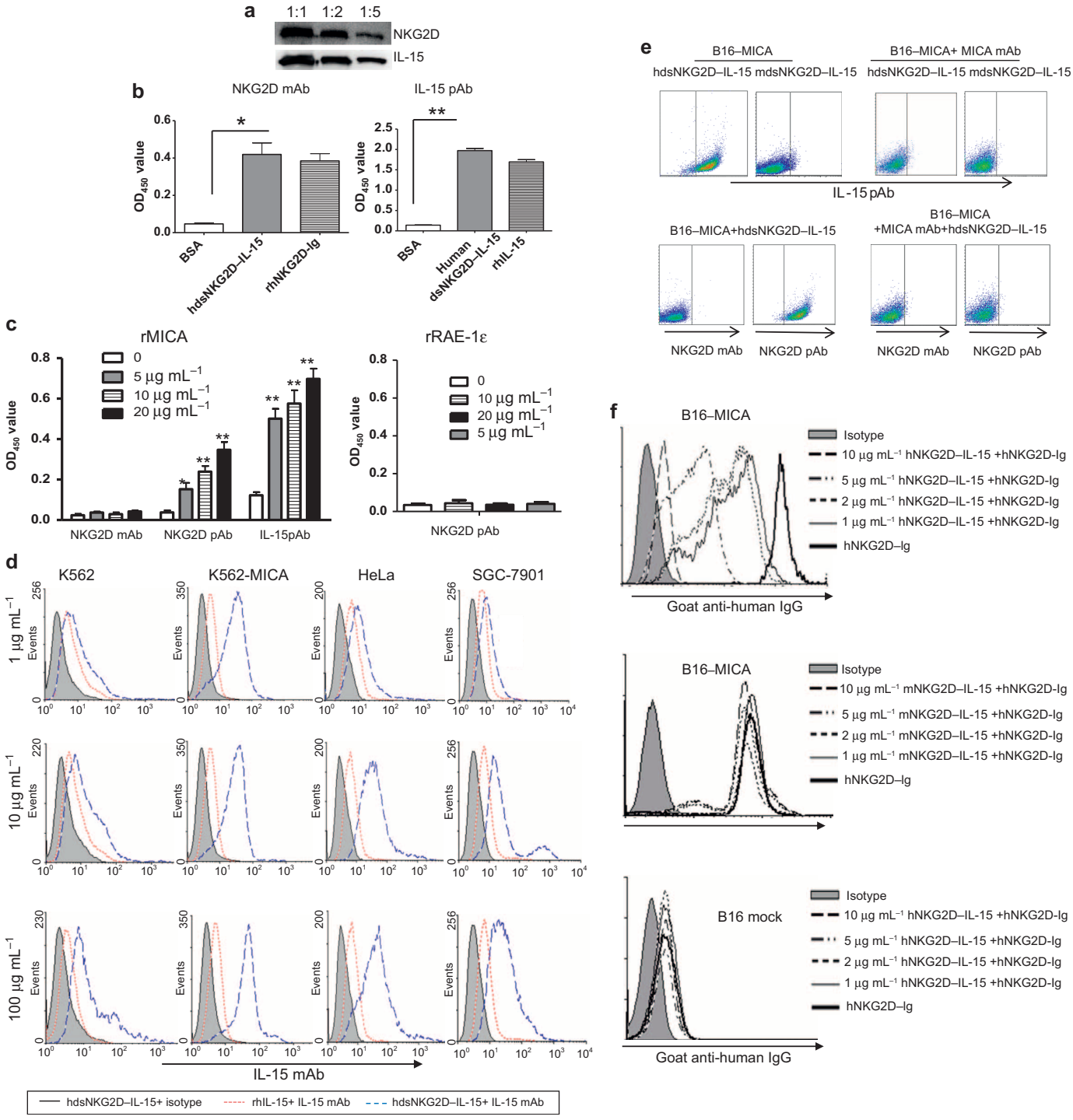

Figure 1 Binding activity of human dsNKG2D–IL-15 with MICA. (**a**) The human dsNKG2D–IL-15 protein was identified by the NKG2D antibody or IL-15 antibody through a western blot assay. (**b**) Plates coated with human dsNKG2D–IL-15, human NKG2D–Ig proteins, and IL-15 were bound by a human NKG2D antibody or an IL-15 antibody and were detected by ELISA. (**c**) Wells were coated with a soluble MICA protein (1 μg) or soluble RAE-1ε (1 μg). Human dsNKG2D–IL-15 was added and incubated at 37°C for 1 h. The NKG2D mAb, NKG2D pAb, or IL-15 pAb and HRP-conjugated secondary antibodies were added sequentially to the wells. The OD 450 value of each well was read after the addition of the substrate and stop solution. (**d**) All tumor cells were incubated with various concentrations of human dsNKG2D–IL-15, stained with a fluorescent IL-15 mAb and detected by flow cytometry. Gray area: isotype control; dotted line: IL-15 (5 μg mL^{-1}) incubation and IL-15 mAb staining; and dashed line: human dsNKG2D–IL-15 incubation and IL-15 mAb staining. (**e**) B16-MICA cells were incubated with human or mouse dsNKG2D–IL-15 and detected with an IL-15 pAb, NKG2D mAb, or NKG2D pAb with or without MICA mAb neutralization. (**f**) B16BL6–MICA cells were co-incubated with serial concentrations of the human dsNKG2D–IL-15, mouse dsNKG2D–IL-15 or human NKG2D–Ig proteins (5 μg mL^{-1}), stained with goat anti-human IgG antibody, and detected by flow cytometry. $^{*}P < 0.05$, $^{**}P < 0.01$.

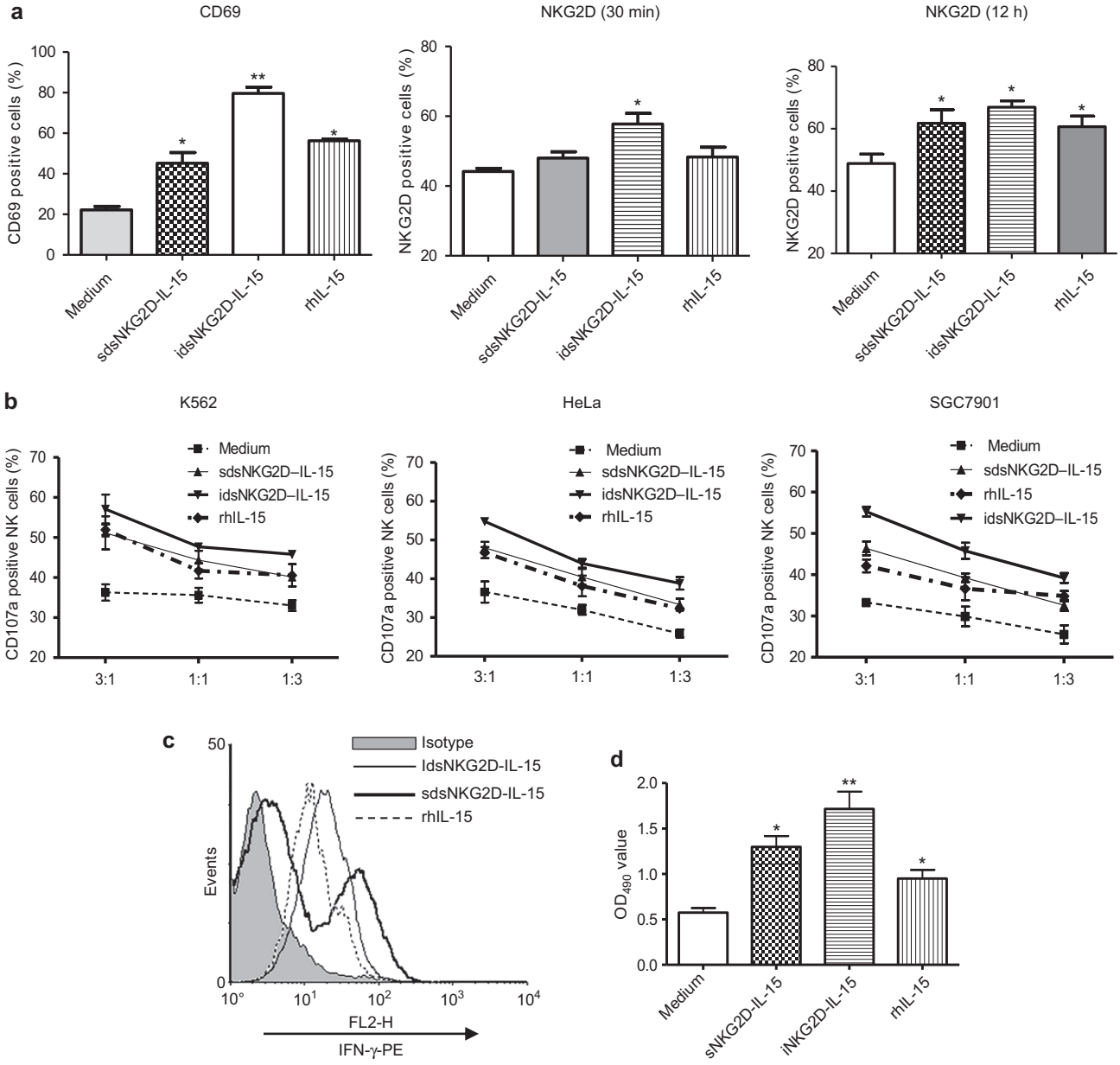

Figure 2 Human dsNKG2D–IL-15 efficiently stimulated CD56$^+$ cells *ex vivo*. (**a**) Frequencies of CD69$^+$ CD56$^+$ cells were detected by flow cytometry following stimulation with soluble, plate-bound human dsNKG2D–IL-15 at the indicated time points. IL-15 was used as a positive control. Stimulation of NKG2D$^+$ CD56$^+$ cells by a variety of conditions were conducted at room temperature for 30 min or at 37°C for 12 h. (**b**) Cytotoxicity of NK cells against K562, HeLa, or SGC-7901 cells stimulated with soluble dsNKG2D–IL-15 and plate-bound dsNKG2D–IL-15 and rhIL-15 was measured by CD107a expression on NK cells. (**c**) IFN-γ production by CD56$^+$ cells was determined with an intracellular staining assay and detected by flow cytometry. (**d**) CD56$^+$ cells sorted using a magnetic bead-labeled antibody were plated (5×10^3) and cultured under various stimulation conditions for 72 h. The expanded cell populations were mixed with MTS/PMS solution, and the absorbance was read at 490 nm. The results are shown as the means ± SD of replicate wells.

B16-MICA cells pre-treated with human dsNKG2D–IL-15, whereas the NKG2D pAb efficiently bound to those cells. Moreover, no binding by the NKG2D pAb was detected following the addition of the MICA antibody (Figure 1e). These results indicated that human dsNKG2D–IL-15 bound to B16-MICA cells through the NKG2D domain.

To confirm that human dsNKG2D–IL-15 recognized membrane-bound MICA, we incubated B16BL6–MICA cells with human NKG2D–Ig alone or human NKG2D–Ig combined with various concentrations of human dsNKG2D–IL-15 or mouse dsNKG2D–IL-15. The binding of NKG2D–Ig with B16BL6–MICA cells decreased as the concentrations of human dsNKG2D–IL-15 proteins increased, as shown by flow cytometry with fluorescence-labeled anti-human IgG. However, mouse dsNKG2D–IL-15 did not affect human NKG2D–Ig binding with the B16-MICA cells, and there was no obvious binding of human

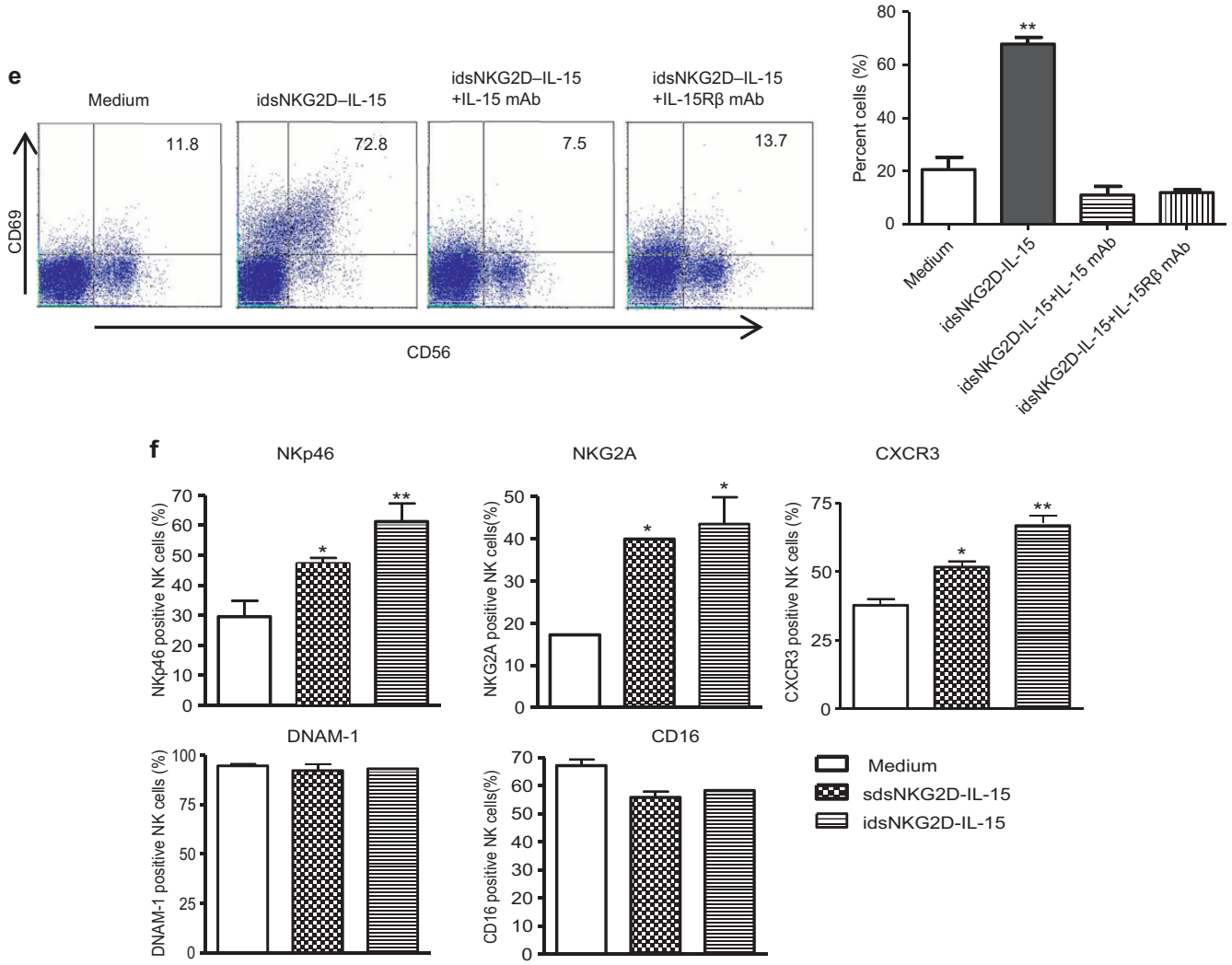

Figure 2 (continued) (**e**) CD69 expression on $CD56^+$ cells stimulated by immobilized hdsNKG2D–IL-15 with IL-15 mAb or simultaneously with IL-15 receptor β blocking. (**f**) All receptors on $CD56^+$ cells with soluble or plate-bound dsNKG2D–IL-15 stimulation were detected using flow cytometry. $*P < 0.05$ versus medium, $**P < 0.01$ versus medium.

NKG2D–Ig with the mock-transfected B16 cells (Figure 1f). Therefore, hdsNKG2D–IL-15 competed with NKG2D–Ig to bind with $MICA^+$ tumor cells through the two NKG2D domains.

Human dsNKG2D–IL-15 proteins efficiently activate NK cells *in vitro*

We assessed the ability of hdsNKG2D–IL-15 to activate NK cells *in vitro*. Similar to IL-15, both soluble and immobilized hdsNKG2D–IL-15 stimulated human $CD56^+$ cells to increase CD69 expression. After a 1-h incubation, only immobilized hdsNKG2D–IL-15 weakly promoted $CD56^+$ cells to express NKG2D. After a 12-h incubation, both soluble and immobilized hdsNKG2D–IL-15 and rhIL-15 all weakly enhanced NKG2D expression (Figure 2a, Supplementary Figure 5a). The cytotoxicities of NK cells against K562, HeLa, and SGC-7901 cells that were pre-stimulated with soluble hdsNKG2D–IL-15, immobilized hdsNKG2D–IL-15, or IL-15 were compared. Both the soluble and immobilized hdsNKG2D–IL-15 proteins highly promoted the killing of the activity, IFN-γ production, and proliferation of NK cells (Figure 2b–d). Additionally, immobilized hdsNKG2D–IL-15 displayed more stimulatory effects (Figure 2a–d).

To confirm that the activation of $CD56^+$ cells by immobilized hdsNKG2D–IL-15 was mediated by the IL-15 domain, an IL-15 conformational antibody was added to wells pre-coated with hdsNKG2D–IL-15 and cultured with human PBMCs overnight. CD69 expression was significantly decreased as compared with stimulation with immobilized hdsNKG2D–IL-15. Additionally, the enhanced expression of CD69 by immobilized hdsNKG2D–IL-15 was completely blocked when an IL-15 receptor β antibody was added to cultured human PBMCs and simultaneously stimulated with immobilized hdsNKG2D–IL-15 (Figure 2e).

Some NK cell receptors were characterized after stimulation with either soluble or immobilized hdsNKG2D–IL-15. As expected, both forms of the hdsNKG2D protein upregulated

NKp46, NKG2A, and CXCR3 expression on $CD56^+$ cells but exhibited no effects on DNAM-1 and CD16 expression levels (Figure 2f, Supplementary Figure 5b). Immobilized hdsNKG2D–IL-15 highly stimulated the expression of NKp46 and CXCR3 on $CD56^+$ cells.

$MICA^+$ tumor cells bound with dsNKG2D–IL-15 stimulate NK cells more efficiently than IL-15

We investigated whether $MICA^+$ tumor cells bound with dsNKG2D–IL-15 had a higher stimulatory effect on NK cell activation than IL-15. Compared with K562–MICA cells alone or K562–MICA cells in combination with IL-15 (K562-$MICA^+$ IL-15), CD69 expression on $CD56^+$ cells was mostly upregulated after stimulation with K562–MICA cells pre-bound with dsNKG2D–IL-15. K562–MICA cells bound with dsNKG2D–IL-15 more efficiently promoted NKG2D expression on $CD56^+$ cells than K562-MICA cell stimulation, but NKG2D expression did not differ from K562-MICA and IL-15 co-stimulation (Figure 3a). No significant difference was observed in NK cytotoxicity against K562 cells pre-incubated with dsNKG2D–IL-15 or IL-15. However, dsNKG2D–IL-15 bound to K562–MICA cells promoted higher cytotoxicity in NK cells than IL-15 pre-incubation with K562–MICA cells. HeLa and SGC-7901 cells pre-bound with dsNKG2D–IL-15 were easily killed by NK cells (Figure 3b). K562–MICA–dsNKG2D–IL-15 cells also stimulated a higher degree of IFN-γ production than stimulation by K562–MICA alone or K562-MICA and IL-15 co-stimulation. The expression of the NKp46 and CXCR3 receptors on NK cells was more enhanced by K562–MICA–dsNKG2D–IL-15 stimulation than K562-MICA and IL-15 co-stimulation. Moreover, CD16 expression on $CD56^+$ cells co-cultured with K562-MICA-dsNKG2D–IL-15 cells was maintained at a higher level compared with K562-MICA and IL-15 co-stimulation. Thus, the membrane-bound dsNKG2D–IL-15 protein could mediate stronger effects on the function of $CD56^+$ cells than IL-15.

Human dsNKG2D–IL-15 inhibits transplanted gastric cancer in nude mice

There is 70% identity between the human and mouse IL-15 proteins. Both human and mouse IL-15 activate mouse NK cells, but mouse IL-15 poorly stimulates human NK cells.[29,30] Human dsNKG2D–IL-15 bound to SGC-7901 cells efficiently, whereas mouse dsNKG2D–IL-15 did not exhibit similar binding activity (Figure 4a). Here, the recombinant mouse dsNKG2D–IL-15 protein was regarded as a soluble form of mouse IL-15 because mouse NKG2D did not bind to the ligands of human NKG2D[25]. Pre-stimulation of mouse NK cells with human dsNKG2D–IL-15 significantly enhanced their killing capacity against SGC-7901 cells. Immobilized dsNKG2D–IL-15 had the most stimulatory effect on NK cells, while soluble dsNKG2D–IL-15 played a role that was similar to recombinant human IL-15 (rhIL-15) (Figure 4b).

To evaluate the anti-tumor activity of human dsNKG2D–IL-15 *in vivo*, we subcutaneously transplanted human gastric cancer cells (SGC-7901) onto the backs of nude mice. Then, human dsNKG2D–IL-15, mouse dsNKG2D–IL-15, or rhIL-15 was injected into the tumor-bearing mice. As expected, human dsNKG2D–IL-15 significantly delayed tumor growth (Figure 4c) and prolonged the lifespan of the tumor-bearing mice (Figure 4d). Mouse dsNKG2D–IL-15 and rhIL-15 also inhibited tumor growth, but their effects were less profound than human dsNKG2D–IL-15. Additionally, mouse dsNKG2D–IL-15 and rhIL-15 mediated similar anti-tumor effects (Figure 4c).We detected mouse NK cells in tumor tissues and spleens of the tumor-bearing nude mice. Compared with the mdsNKG2D–IL-15 and rhIL-15 treatments, human dsNKG2D–IL-15 highly enhanced mouse NK and $NKG2D^+$ NK cell frequencies in tumor tissues (Figure 4e, Supplementary Figure 6). Although splenic NK and $NKG2D^+$ NK cell frequencies were higher after treatment with human dsNKG2D–IL-15 than mouse dsNKG2D–IL-15, there was no significant difference between treatment with human dsNKG2D–IL-15 and rhIL-15 (Figure 4f, Supplementary Figure 6). Thus, the fused human dsNKG2D–IL-15 protein exhibited a superior ability to recruit NK cells into tumor tissues compared with IL-15.

Human dsNKG2D–IL-15 recruits NK cells to xenografted gastric cancers in nude mice

The accumulation of human dsNKG2D–IL-15 in tumor tissues was assessed by *in vivo* imaging technology. Human dsNKG2D–IL-15 pre-labeled with Cy5.5 fluorescein was injected into the tail-vein of a tumor-bearing mouse. Approximately 4–8 h later, fluorescent proteins were observed at the tumor tissue sites (Figure 5a). Next, we analyzed whether hdsNKG2D–IL-15 treatment directly recruited $CD56^+$ cells to the tumor sites. SGC-7901 cells were transplanted into nude mice that were depleted of $NK1.1^+$ cells. When tumors were easily detected, human PBMCs were stained with a fluorescent dye (carboxyfluorescein succinimidyl ester) and intravenously injected into the tumor-bearing mice. The frequencies of transplanted human $CD56^+$ cells in the tumor tissues and spleens of the nude mice were measured. In the solid tumors, human dsNKG2D–IL-15 enhanced the recruitment of $CD56^+$ cells compared with mouse dsNKG2D–IL-15 and rhIL-15. However, there was no significant difference in the $CD56^+$ cell frequency in the spleen between mice treated with human dsNKG2D–IL-15 and rhIL-15. This result indicates that human dsNKG2D–IL-15 could promote the migration of $CD56^+$ cells to tumor tissues (Figure 5b).

Anti-tumor activity of hdsNKG2D–IL-15 mostly depends on NK cells

We analyzed the anti-tumor activity and the cellular mechanisms of human dsNKG2D–IL-15 in normal C57BL/6 mice. B16BL6–MICA and B16BL6 cells were subcutaneously transplanted into C57BL/6 mice. Then, the human and mouse dsNKG2D–IL-15 proteins were intraperitoneally injected into the tumor-bearing mice. Human dsNKG2D–IL-15 and mdsNKG2D–IL-15 both suppressed tumor growth in the

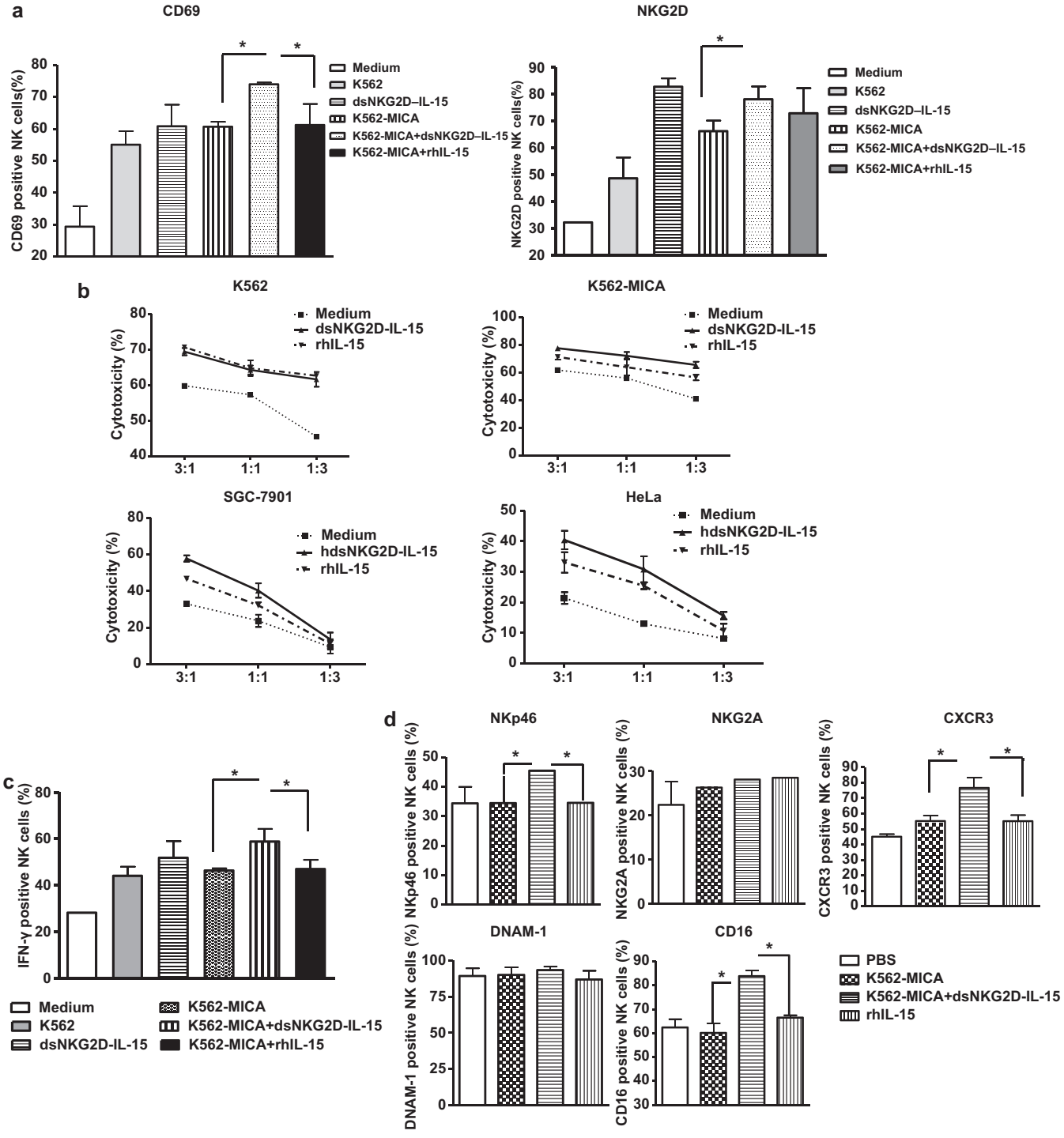

Figure 3 Membrane-bound human dsNKG2D–IL-15 had stronger stimulatory effects than IL-15. (**a**) Frequencies of $CD69^+$ NK cells and $NKG2D^+$ NK cells were detected by flow cytometry; then, the cells were cultured under various stimulation conditions. For K562–MICA+dsNKG2D–IL-15 treatment, K562–MICA cells were incubated with the human dsNKG2D–IL-15 (10 $\mu g\,mL^{-1}$) proteins at 37°C for 1 h, washed, and cultured with NK cells. (**b**) Human dsNKG2D–IL-15 was pre-incubated with $MICA^+$ tumor cells. The washed tumor cells bound to dsNKG2D–IL-15 cells were mixed with NK cells. IL-15 was also added to the cell cultures when the NK cells were mixed with the $MICA^+$ tumor cells. Cytotoxicity was determined by variations in CD107a expression. (**c**) IFN-γ production was detected by intracellular staining and flow cytometry. (**d**) All receptors on NK cells were detected by flow cytometry following a variety of stimulations. $*P < 0.05$, $**P < 0.01$.

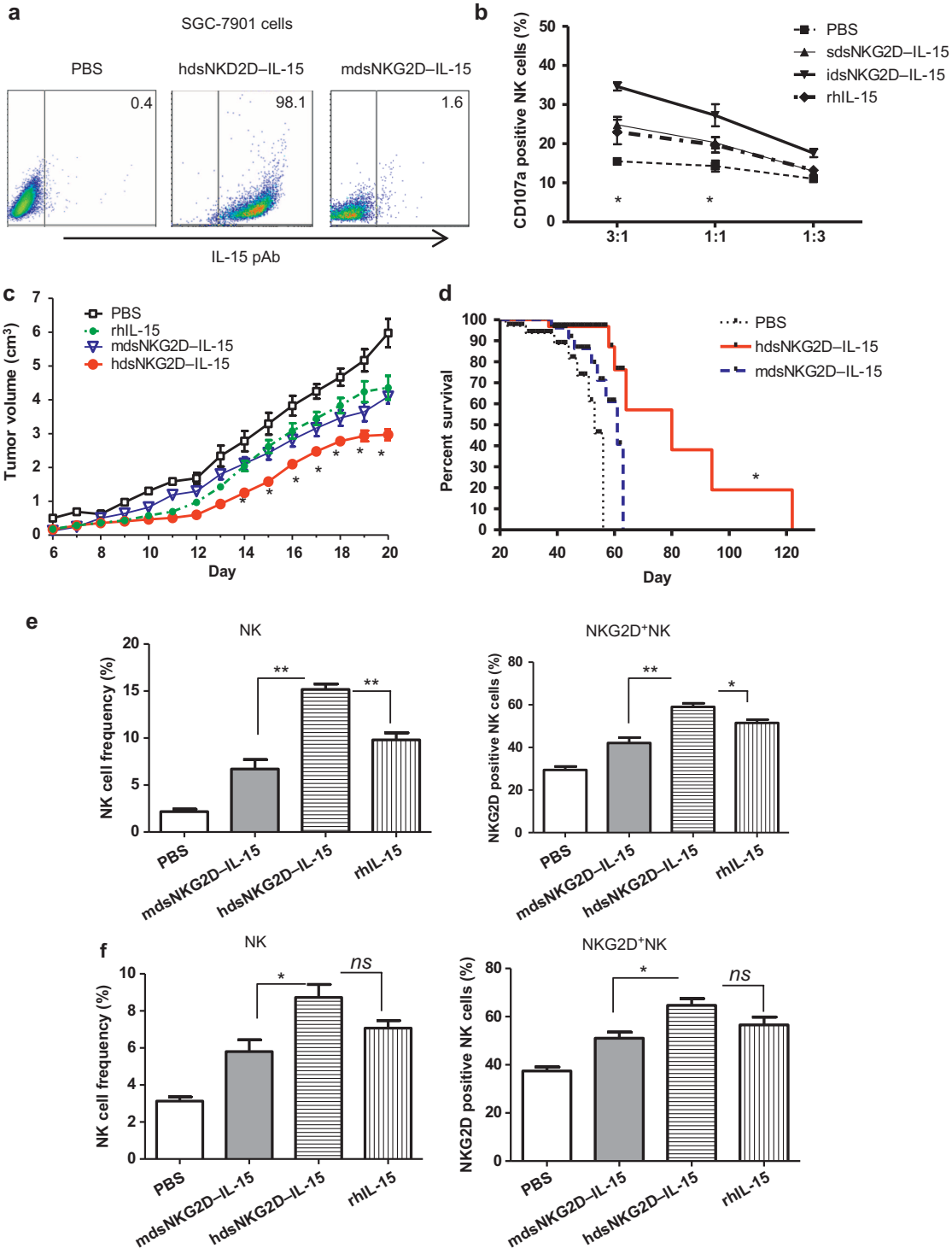

Figure 4 Human dsNKG2D–IL-15 inhibits transplanted gastric cancer in nude mice. (**a**) Human or mouse dsNKG2D–IL-15 was incubated with SGC-7901 cells and stained with the IL-15 pAb. (**b**) Mouse NK cell degranulation against SGC-7901 cells stimulated by soluble or immobilized human dsNKG2D–IL-15 or rhIL-15 was detected by CD107a mAb staining. (**c**) Human gastric cancer cells (SGC-7901, 2×10^6 cells) were subcutaneously injected into the backs of nude mice ($n = 6$) on day 0. Either human dsNKG2D–IL-15 (60 μg), mouse dsNKG2D–IL-15 (60 μg), rhIL-15 (60 μg), or PBS was intraperitoneally injected daily into these mice from days 6 to 20. Tumor dimensions were measured, and volumes were calculated and are shown as the means ± SD. (**d**) Reagents were injected into tumor-bearing mice from days 5 to 21. Then, the mice were fed normally, and mouse deaths were documented over time. The data are presented in Kaplan–Meier survival curves. Asterisks represent comparison between human dsNKG2D–IL-15 and rhIL-15 treatments. Frequencies of NK cells and the percentages of $NKG2D^+$ NK cells in tumor tissues (**e**) and spleens (**f**) from cancer-bearing mice on day 21, as determined by flow cytometry ($n = 4$). $^*P < 0.05$, $^{**}P < 0.01$, *ns* means no significance. The experiments were performed twice.

B16BL6–MICA cell-transplanted mice, but human dsNKG2D–IL-15 played a more significant role. In the B16BL6 cell-transplanted mice, the two recombinant proteins mediated similar effects in the retardation of tumor growth (Figure 6a). The tumor-bearing mice treated with the two types of dsNKG2D–IL-15 also showed no signs of inflammatory damages (e.g., diarrhea, skin rash, and ruffled hair), suggesting an absence of toxicity.

Frequencies of $NKG2D^+$ NK cells (Figure 6b), $CD8^+$ $NKG2D^+$ T cells, and $CD8^+CD44^+$ T cells (Figure 6c) in the spleen were significantly higher in mice that received human dsNKG2D–IL-15 treatment than in B16BL6–MICA-bearing mice treated with PBS and mdsNKG2D–IL-15. CD44 mediates the recruitment of lymphocytes to sites of inflammation, and its enhanced expression represents cell activation. Only the $CD8^+NKG2D^+$ T-cell frequency was enhanced following human or mouse dsNKG2D–IL-15 treatment compared with PBS treatment in the B16-bearing mice (Supplementary Figure 7). Moreover, when NK cells were depleted in the B16BL6–MICA bearing mice prior to the injection of the recombinant human dsNKG2D–IL-15 protein, the anti-melanoma effects induced by human dsNKG2D–IL-15 were significantly blocked. By contrast, melanoma growth in mice subjected to $CD8^+$ T-cell depletion was faster only on days 16–18 compared with mice treated with human dsNKG2D–IL-15 alone (Figure 6d). Thus, NK cell activation by human dsNKG2D–IL-15 was the primary contributor to tumor inhibition *in vivo*.

DISCUSSION

We generated a fusion protein (human dsNKG2D–IL-15) that bridged $MICA^+$ tumor cells and IL-15 receptor $\beta\gamma^+$ lymphocytes to mediate anti-tumor activities. The recombinant human dsNKG2D–IL-15 could efficiently bind to $MICA^+$ tumor cells and stimulate NK cell activity by trans-presentation of IL-15. The human dsNKG2D–IL-15 protein accumulated in tumor tissues and inhibited the growth of gastric cancers following transplantation of SGC-7901 cells into nude mice; additionally, human dsNKG2D–IL-15 prolonged the survival of tumor-bearing mice. Enhancement of NK cell activation and recruitment by dsNKG2D–IL-15 contributed to tumor inhibition. The suppressive effects of human dsNKG2D–IL-15 against B16BL6–MICA-tumor mice were primarily dependent on the activation of NK cells. Thus, recombinant human dsNKG2D–IL-15 could be regarded as a potential new reagent for use in $MICA^+$ tumor patients.

MICA is a signal of stress and is highly expressed on tumor cells at an early state.[31] Ectopic expression of MICA on tumor cells stimulated NK cell activation and thus promoted anti-tumor activity.[32,33] However, the tumor environment is complicated. First, tumor cells with high level expression of MICA or other NKG2D ligands were killed as the tumor developed. Only tumor cells with low-level expression of the NKG2D ligands survived *in vivo*.[34] Second, MICA was shed from tumor cells by the ADAM protease[35] or metalloproteinases.[36] Serum NKG2D ligands not only competed with the membrane proteins for NKG2D binding but also downregulated NKG2D expression on lymphocytes.[37] Third, the persistent expression of MICA on dendritic cells or tumor cells induced regulatory $CD4^+NKG2D^+$ T cells to promote tumor evasion by expressing membrane-bound TGF-β and the Fas ligand.[38,39] Thus, the human dsNKG2D–IL-15 protein may not only bind to tumor cells but also potentially neutralize serum NKG2D ligands.

The use of dsNKG2D–IL-15 for tumor treatment also has other advantages. The molecular weight of dsNKG2D–IL-15 was $<$50 kD, indicating that this molecule could easily penetrate into tumor tissues. Because both the NKG2D and IL-15 domains of dsNKG2D–IL-15 were the same as those of endogenous human NKG2D and IL-15, the fusion protein was weakly immunogenic. IL-15 also upregulated NKG2D expression levels on lymphocytes to promote anti-tumor activity.[40] Furthermore, some pharmaceutical anti-tumor agents (e.g., doxorubicin[41] and histone deacetylase inhibitors[42]) induced MICA expression on tumor cells. Combined therapy of such drugs and dsNKG2D–IL-15 had strong anti-tumor effects.

The IL-15 receptor α (IL-15 Rα) trans-presents IL-15 on monocytes and dendritic cells; IL-15 Rα is redundant for IL-15 binding.[12,14] IL-15 Rα is also expressed on some epithelial cells[43] and has potential activity for exogenous IL-15 binding. There was no significant binding of IL-15 to $MICA^+$ cells based on rhIL-15 incubation and subsequent IL-15 mAb staining (Figure 1c, red dotted line), indicating that exogenous IL-15 did not bind membrane-bound IL-15 Rα. The addition of an anti-MICA neutralizing mAb completely blocked human dsNKG2D–IL-15 binding to B16-MICA cells. This result also confirmed that dsNKG2D–IL-15 bound to $MICA^+$ cells via the NKG2D domain and not the IL-15 domain.

B16BL6–MICA cells bound to human dsNKG2D–IL-15 and could imitate IL-15 trans-presentation to activate NK and $CD8^+$ T cells. The stronger anti-tumor effect following injection of human dsNKG2D–IL-15 in B16BL6–MICA-tumor mice was not due to the higher stimulatory activity of human dsNKG2D–IL-15 compared with mdsNKG2D–IL-15. We previously reported that human dsNKG2D–IL-15 was weaker than mdsNKG2D–IL-15 in suppressing tumor growth in CT-26-transplanted tumor mice.[26] Human NK cell migration to the transplanted gastric cancers was regarded as the subsequent event following NK cell activation. Human dsNKG2D–IL-15 stimulates NK cells to produce IFN-γ, and IFN-γ production by activated NK cells stimulates the secretion of CXCR3 ligands such as IP-10 in tumor cells.[44] Furthermore, both the soluble and membrane-bound dsNKG2D–IL-15 proteins directly upregulated CXCR3 expression on NK cells, as shown in the results (Figure 2e and 3d).

There was a possibility that dsNKG2D–IL-15 would compete with the interaction of MICA on cancer cells and NKG2D on NK cells and thus downregulate NK cell activation. However, the NKG2D expression level on NK cells was low in advanced tumor patients and NK cell function was generally inhibited.[45] The affinity of IL-15 and its receptor βγ ($Kd \sim 10^{-9}$ M)[46] was significantly higher than the affinity between

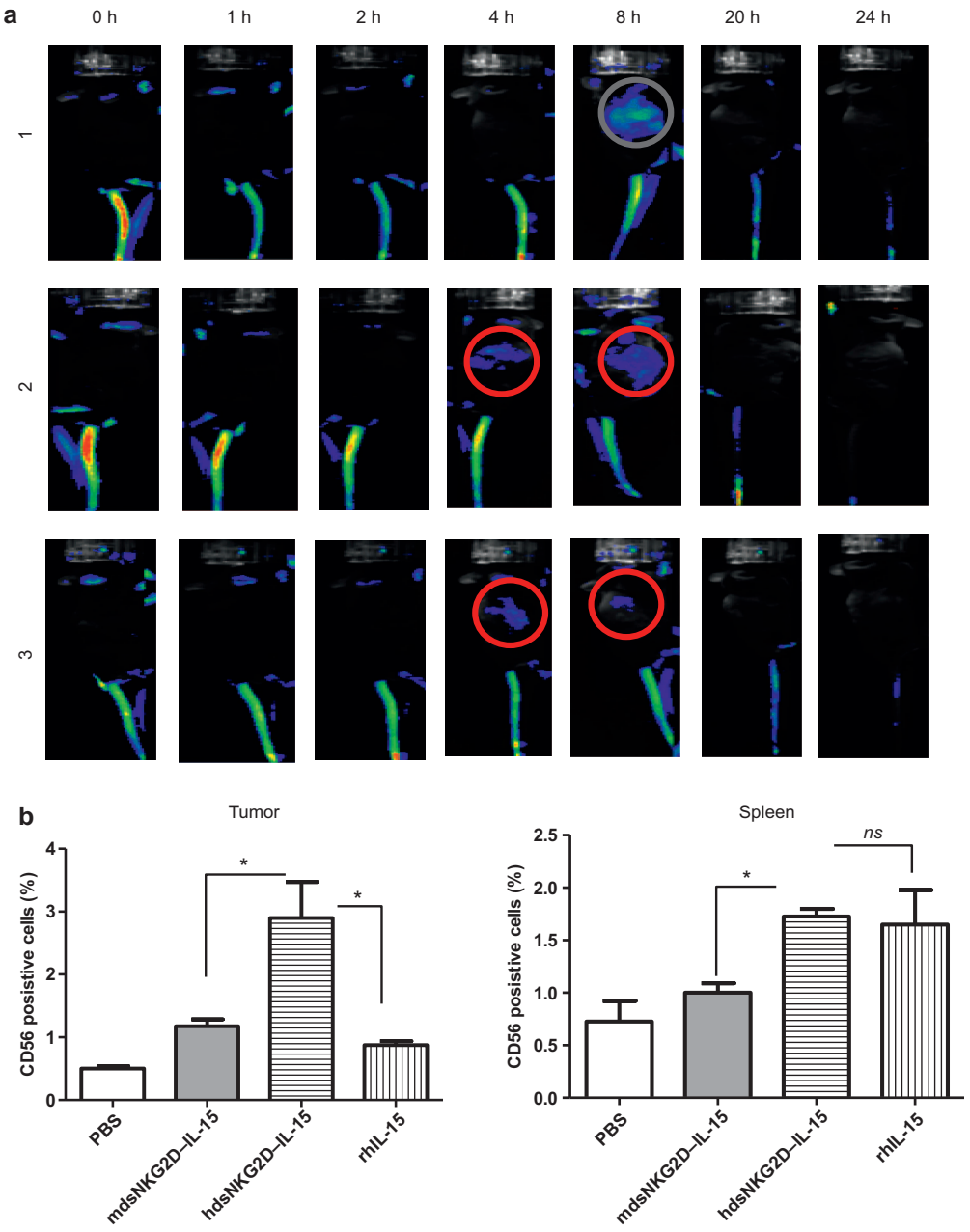

Figure 5 Human dsNKG2D–IL-15 recruited NK cells to tumor tissues. (**a**) Ten days after B16-MICA cells were subcutaneously injected into the backs of C57BL6 mice, Cy5.5-labled hdsNKG2D–IL-15 (80 μg) was injected into the tail veins. Fluorescent signals in three mice were documented at the indicated times. (**b**) Rabbit polyclonal anti-asialo-GM1 antibody was intraperitoneally injected into nude mice (100 μg) every 3 d. After SGC7901 cells transplanted in nude mice ($n = 4$) formed visible tumors, human dsNKG2D–IL-15, mouse dsNKG2D–IL-15, or rhIL-15 (60 μg) was intraperitoneally injected. After 0.5 h, human PBMCs pre-stained with CFSE (5×10^6) were intravenously injected into the nude mice. Six hours later, the mice were killed and their spleens and tumor tissues were collected. The frequencies of $CD56^+$ cells in tumor tissues and spleens were detected by flow cytometry.*$P < 0.05$, *ns* means no significance. The experiments were performed three times.

MICA and NKG2D ($Kd \sim 10^{-6}$ M).[47] Thus, the addition of IL-15 would be theoretically more effective for NK cell activation in tumor patients than NKG2D ligation. The anti-tumor activity shown by dsNKG2D–IL-15 in our study confirmed the effective activation of NK cells by dsNKG2D–IL-15.

A fusion protein composed of the NH_2-terminal (amino acids 1–77) sushi domain of IL-15 receptor α coupled via a linker to IL-15 displayed better efficacy than IL-15 *in vitro*.[9] An antibody-cytokine fusion protein (scFv_RD_IL-15) was composed of an antibody moiety targeting the tumor stromal fibroblast activation protein and an extended IL-15Rα sushi domain (RD); the IL-15 in this protein exhibited antibody-mediated specific binding and cytokine activity. The scFv_RD_IL-15fusion protein showed a superior anti-tumor

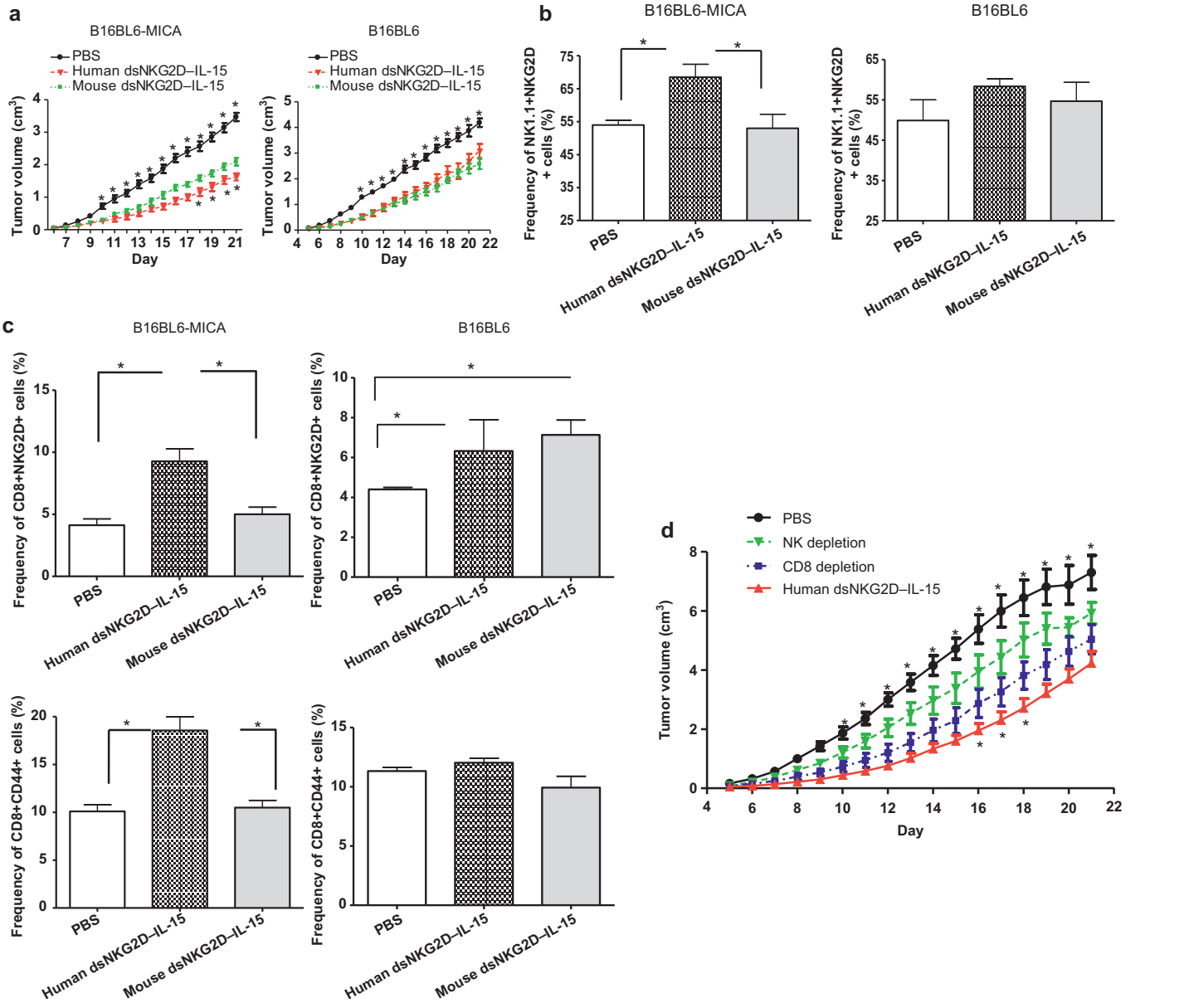

Figure 6 Anti-tumor effects of human dsNKG2D–IL-15depended mainly on NK cells. (**a**) B16BL6–MICA or B16 cells were injected into the C57BL/6 mice ($n = 6$, 2×10^6 cells). Human dsNKG2D–IL-15 (60 μg), mouse dsNKG2D–IL-15 (60 μg), or PBS was also intraperitoneally injected daily into these mice from days 5 to 21. Tumor growth was measured daily and was shown as the means ± SD. The upper asterisks represent the comparison between human dsNKG2D–IL-15 and PBS, and the lower asterisks represent the comparison between human dsNKG2D–IL-15 and mouse dsNKG2D–IL-15. All mice were killed on day 22, and their spleens were collected. The frequencies of splenic $NK1.1^+NKG2D^+$ cells (**b**), $CD8^+NKG2D^+$ T cells and $CD8^+CD44^+$ T cells (**c**) were detected by flow cytometry. $^*P < 0.05$, $^{**}P < 0.01$. (**d**) Growth curve of B16-MICA transplanted tumors in mice treated with human dsNKG2D–IL-15 from day 5 following either NK or $CD8^+$ T cell depletion ($n = 5$). The upper asterisks represent the comparison between human dsNKG2D–IL-15 and NK cell depletion, and the lower asterisks represent the comparison between human dsNKG2D–IL-15 and $CD8^+$ T-cell depletion. The experiments were performed twice.

effect compared with the effect induced by an untargeted or RD-missing version of the IL-15 fusion protein.[10,20] However, whether the addition of the IL-15Rα sushi domain in the dsNKG2D–IL-15 protein also has synergistic effects needs further study.

In conclusion, the recombinant human dsNKG2D–IL-15 protein mediated tumor-specific binding and IL-15 activity. The membrane-bound fusion protein showed stronger effects than IL-15 *in vitro* and *in vivo*. Following more detailed pharmacokinetic analysis *in vivo*, human dsNKG2D–IL-15 could be used as a potential adjuvant to activate NK cells and $CD8^+$ T cells for tumor therapy.

DISCLOSURES

All authors have declared there are no financial conflicts of interest with regard to this work.

ACKNOWLEDGEMENTS

This work was supported by the National Natural Science Foundation (nos. 81172785 and 81471547), the Natural Science Fund of Jiangsu Province (BK2011449 and BK2008215), and the collaborative fund of Yangzhou University and Yangzhou municipality (2012038-5).

Supplementary information of this article can be found on the *Cellular & Molecular Immunology*'s website (http://www.nature.com/cmi).

1 Steel JC, Waldmann TA, Morris JC. Interleukin-15 biology and its therapeutic implications in cancer. *Trends Pharmacol Sci* 2012; **33**: 35–41.
2 Jakobisiak M, Golab J, Lasek W. Interleukin 15 as a promising candidate for tumor immunotherapy. *Cytokine Growth Factor Rev* 2011; **22**: 99–108.
3 Sanjabi S, Mosaheb MM, Flavell RA. Opposing effects of TGF-beta and IL-15 cytokines control the number of short-lived effector $CD8^+$ T cells. *Immunity* 2009; **31**: 131–144.
4 Tao Q, Chen T, Tao L, Wang H, Pan Y, Xiong S *et al*. IL-15 improves the cytotoxicity of cytokine-induced killer cells against leukemia cells by upregulating $CD3^+CD56^+$ cells and downregulating regulatory T cells as well as IL-35. *J Immunother* 2013; **36**: 462–467.
5 Berger C, Berger M, Hackman RC, Gough M, Elliott C, Jensen MC *et al*. Safety and immunologic effects of IL-15 administration in nonhuman primates. *Blood* 2009; **114**: 2417–2426.
6 Imamura M, Shook D, Kamiya T, Shimasaki N, Chai SM, Coustan-Smith E *et al*. Autonomous growth and increased cytotoxicity of natural killer cells expressing membrane-bound interleukin-15. *Blood* 2014; **124**: 1081–1088.
7 Yiang GT, Chou RH, Chang WJ, Wei CW, Yu YL. Long-term expression of rAAV2-hIL15 enhances immunoglobulin production and lymphokine-activated killer cell-mediated human glioblastoma cell death. *Mol Clin Oncol* 2013; **1**: 321–325.
8 Zhao DX, Li ZJ, Zhang Y, Zhang XN, Zhao KC, Li YG *et al*. Enhanced antitumor immunity is elicited by adenovirus-mediated gene transfer of CCL21 and IL-15 in murine colon carcinomas. *Cell Immunol* 2014; **289**: 155–161.
9 Bessard A, Solé V, Bouchaud G, Quéméner A, Jacques Y. High antitumor activity of RLI, an interleukin-15 (IL-15)-IL-15 receptor alpha fusion protein, in metastatic melanoma and colorectal cancer. *Mol Cancer Ther* 2009; **8**: 2736–2745.
10 Kermer V, Baum V, Hornig N, Kontermann RE, Müller D. An antibody fusion protein for cancer immunotherapy mimicking IL-15 trans-presentation at the tumor site. *Mol Cancer Ther* 2012; **11**: 1279–1288.
11 Cheever MA. Twelve immunotherapy drugs that could cure cancers. *Immunol Rev* 2008; **222**: 357–368.
12 Müller JR, Waldmann TA, Kruhlak MJ, Dubois S. Paracrine and trans-presentation functions of IL-15 are mediated by diverse splice versions of IL-15Rα in human monocytes and dendritic cells. *J Biol Chem* 2012; **287**: 40328–40338.
13 Lucas M, Schachterle W, Oberle K, Aichele P, Diefenbach A. Dendritic cells prime natural killer cells by trans-presenting interleukin 15. *Immunity* 2007; **26**: 503–517.
14 Castillo EF, Schluns KS. Regulating the immune system via IL-15 trans-presentation. *Cytokine* 2012; **59**: 479–490.
15 Huntington ND, Alves NL, Legrand N, Lim A, Strick-Marchand H, Mention JJ *et al*. IL-15 trans-presentation promotes both human T-cell reconstitution and T-cell-dependent antibody responses *in vivo*. *Proc Natl Acad Sci USA* 2011; **108**: 6217–6222.
16 Kobayashi H, Dubois S, Sato N, Sabzevari H, Sakai Y, Waldmann TA *et al*. Role of trans-cellular IL-15 presentation in the activation of NK cell-mediated killing, which leads to enhanced tumor immunosurveillance. *Blood* 2005; **105**: 721–727.
17 Stoklasek TA, Schluns KS, Lefrançois L. Combined IL-15/IL-15Ralpha immunotherapy maximizes IL-15 activity *in vivo*. *J Immunol* 2006; **177**: 6072–6080.
18 Dubois S, Patel HJ, Zhang M, Waldmann TA, Müller JR. Preassociation of IL-15 with IL-15R alpha-IgG1-Fc enhances its activity on proliferation of NK and $CD8^+/CD44^{high}$ T cells and its antitumor action. *J Immunol* 2008; **180**: 2099–2106.
19 Waldmann TA, Conlon KC, Stewart DM, Worthy TA, Janik JE, Fleisher TA *et al*. Phase 1 trial of IL-15 trans presentation blockade using humanized Mikβ1 mAb in patients with T-cell large granular lymphocytic leukemia. *Blood* 2013; **121**: 476–484.
20 Bouchaud G, Garrigue-Antar L, Solé V, Quéméner A, Boublik Y, Mortier E *et al*. The exon-3-encoded domain of IL-15R alpha contributes to IL-15 high-affinity binding and is crucial for the IL-15 antagonistic effect of soluble IL-15Ralpha. *J Mol Biol* 2008; **382**: 1–12.
21 Ullrich E, Koch J, Cerwenka A, Steinle A. New prospects on the NKG2D/NKG2DL system for oncology. *Oncoimmunology* 2013; **2**: e26097.
22 Wu J, Song Y, Bakker AB, Bauer S, Spies T, Lanier LL *et al*. An activating immunoreceptor complex formed by NKG2D and DAP10. *Science* 1999; **285**: 730–732.
23 Hayakawa Y. Targeting NKG2D in tumor surveillance. *Expert Opin Ther Targets* 2012; **16**: 587–599.
24 Salih HR, Holdenrieder S, Steinle A. Soluble NKG2D ligands: prevalence, release, and functional impact. *Front Biosci* 2008; **13**: 3448–3456.
25 Zhang T, Sentman CL. Cancer immunotherapy using a bispecific NK receptor fusion protein that engages both T cells and tumor cells. *Cancer Res* 2011; **71**: 2066–2076.
26 Xia Y, Chen B, Shao X, Xiao W, Qian L, Ding Y *et al*. Treatment with a fusion protein of the extracellular domains of NKG2D to IL-15 retards colon cancer growth in mice. *J Immunother* 2014; **37**: 257–266.
27 Gong W, Xiao W, Hu M, Weng X, Qian L, Pan X *et al*. *Ex vivo* expansion of natural killer cells with high cytotoxicity by K562 cells modified to co-express major histocompatibility complex class I chain-related protein A, 4-1BB ligand, and interleukin-15. *Tissue Antigens* 2010; **76**: 467–475.
28 Lin Z, Wang C, Xia H, Liu W, Xiao W, Qian L *et al*. CD4(+) NKG2D(+) T cells induce NKG2D down-regulation in natural killer cells in CD86-RAE-1ε transgenic mice. *Immunology* 2014; **141**: 401–415.
29 Mrózek E, Anderson P, Caligiuri MA. Role of interleukin-15 in the development of human $CD56^+$ natural killer cells from $CD34^+$ hematopoietic progenitor cells. *Blood* 1996; **87**: 2632–2640.
30 Barao I, Alvarez M, Redelman D, Weiss JM, Ortaldo JR, Wiltrout RH *et al*. Hydrodynamic delivery of human IL-15 cDNA increases murine natural killer cell recovery after syngeneic bone marrow transplantation. *Biol Blood Marrow Transplant* 2011; **17**: 1754–1764.
31 Bauer S, Groh V, Wu J, Steinle A, Phillips JH, Lanier LL *et al*. Activation of NK cells and T cells by NKG2D, a receptor for stress-inducible MICA. *Science* 1999; **285**: 727–729.
32 Cerwenka A, Baron JL, Lanier LL. Ectopic expression of retinoic acid early inducible-1 gene (RAE-1) permits natural killer cell-mediated rejection of a MHC class I-bearing tumor *in vivo*. *Proc Natl Acad Sci USA* 2001; **98**: 11521–11526.
33 Diefenbach A, Jensen ER, Jamieson AM, Raulet DH. Rae1 and H60 ligands of the NKG2D receptor stimulate tumour immunity. *Nature* 2001; **413**: 165–171.
34 Zhang J, Xu Z, Zhou X, Zhang H, Yang N, Wu Y *et al*. Loss of expression of MHC class I-related chain A (MICA) is a frequent event and predicts poor survival in patients with hepatocellular carcinoma. *Int J Clin Exp Pathol* 2014; **7**: 3123–3231.
35 Chitadze G, Lettau M, Bhat J, Wesch D, Steinle A, Fürst D *et al*. Shedding of endogenous MHC class I-related chain molecules A and B from different human tumor entities: heterogeneous involvement of the "a disintegrin and metalloproteases" 10 and 17. *Int J Cancer* 2013; **133**: 1557–1566.
36 Kaiser BK, Yim D, Chow IT, Gonzalez S, Dai Z, Mann HH *et al*. Disulphide-isomerase-enabled shedding of tumor-associated NKG2D ligands. *Nature* 2007; **447**: 482–486.
37 Chitadze G, Bhat J, Lettau M, Janssen O, Kabelitz D. Generation of soluble NKG2D ligands: proteolytic cleavage, exosome secretion and functional implications. *Scand J Immunol* 2013; **78**: 120–129.

38 Dai Z, Turtle CJ, Booth GC, Riddell SR, Gooley TA, Stevens AM *et al*. Normally occurring NKG2D+CD4+ T cells are immunosuppressive and inversely correlated with disease activity in juvenile-onset lupus. *J Exp Med* 2009; **206**: 793–805.
39 Groh V, Smythe K, Dai Z, Spies T. Fas-ligand-mediated paracrine T cell regulation by the receptor NKG2D in tumor immunity. *Nat Immunol* 2006; **7**: 755–762.
40 Zhang C, Zhang J, Niu J, Zhang J, Tian Z. Interleukin-15 improves cytotoxicity of natural killer cells via up-regulating NKG2D and cytotoxic effector molecule expression as well as STAT1 and ERK1/2 phosphorylation. *Cytokine* 2008; **42**: 128–136.
41 Soriani A, Zingoni A, Cerboni C, Iannitto ML, Ricciardi MR, Di Gialleonardo V *et al*. ATM-ATR-dependent up-regulation of DNAM-1 and NKG2D ligands on multiple myeloma cells by therapeutic agents results in enhanced NK-cell susceptibility and is associated with a senescent phenotype. *Blood* 2009; **113**: 3503–3511.
42 Diermayr S, Himmelreich H, Durovic B, Mathys-Schneeberger A, Siegler U, Langenkamp U *et al*. NKG2D ligand expression in AML increases in response to HDAC inhibitor valproic acid and contributes to allorecognition by NK-cell lines with single KIR-HLA class I specificities. *Blood* 2008; **111**: 1428–1436.
43 Bouchaud G, Gehrke S, Krieg C, Kolios A, Hafner J, Navarini AA *et al*. Epidermal IL-15Rα acts as an endogenous antagonist of psoriasiform inflammation in mouse and man. *J Exp Med* 2013; **210**: 2105–2117.
44 Wendel M, Galani IE, Suri-Payer E, Cerwenka A. Natural killer cell accumulation in tumors is dependent on IFN-gamma and CXCR3 ligands. *Cancer Res* 2008; **68**: 8437–8445.
45 González S, Groh V, Spies T. Immunobiology of human NKG2D and its ligands. *Curr Top Microbiol Immunol* 2006; **298**: 121–138.
46 Giri JG, Kumaki S Ahdieh M Friend DJ, Loomis A, Shanebeck K *et al*. Identification and cloning of a novel IL-15 binding protein that is structurally related to the alpha chain of the IL-2 receptor. *EMBO J* 1995; **14**: 3654–3663.
47 Raulet DH, Gasser S, Gowen BG, Deng W, Jung H. Regulation of ligands for the NKG2D activating receptor. *Annu Rev Immunol* 2013; **31**: 413–441.